Exp Brain Res (1996) 110:248–264

RESEARCH ARTICLE

J. McIntyre · F.A. Mussa-Ivaldi · E. Bizzi

The control of stable postures in the multijoint arm

Received: 1 August 1994 / Accepted: 20 November 1995

Abstract The stiffness that is measured at the hand of a multijoint arm emerges from the combined effects of the elastic properties of the muscles and joints, the geometry of the linkages and muscle attachments, and the neural control circuits that act on the arm. The effective stiffness of a nonlinear linkage such as a two-joint arm depends on the force acting on the system as well as the intrinsic stiffness of the actuators. This paper presents an analysis of the factors that affect limb stiffness, including the effects of external forces. Three potential strategies for controlling the stability of the limb are proposed and demonstrated by computer simulations. The predictions from the simulations are then compared experimentally with measured stiffness values for human subjects working against an external force. These experiments were directed toward understanding what strategies are used by the CNS to control limb stiffness and stability. The experimental evidence showed that human subjects *must* increase the stiffness at the joints in order to maintain limb stability in the presence of applied external forces at the hand. In the process we identified a precise role for muscles which span two or more joints in the control of overall limb stiffness. A local strategy may be used to achieve limb stability, in which the muscle stiffness increases with muscle force. Multijoint muscles are shown to provide mechanical couplings which are necessary for the maintenance of stability. By utilizing these muscles, the neuro-musculo-skeletal system can control a global property of the system (stability) with a passive local strategy.

J. McIntyre[1] · F.A. Mussa-Ivaldi[2] · E. Bizzi(✉)[3]
Department of Brain and Cognitive Sciences,
Massachusetts Institute of Technology, E25-534,
Cambridge, MA 02139-4307, USA

Present addresses:
[1] LPPA/CNRS – Collège de France,
15 rue de l'Ecole de Médecine, 75270 Paris Cedex 06, France
[2] Department of Physiology and
Department of Physical Medicine and Rehabilitation,
Northwestern University Medical School, Chicago, Ill 60611, USA
[3] Sez. Ricerche Fisiologia Umana, CNR, Clinica S. Lucia,
via Ardeatina, 306, I-00179 Rome, Italy;
Fax: +39-6-51-50-14-77; e-mail: jam@ccr.jussieu.fr

Key words Stiffness · Impedance · Stability · Posture · Motor control · Human

Introduction

When constrained to act in the horizontal plane, the human arm is known to behave at the endpoint like a two-dimensional spring (Hogan 1985; Mussa-Ivaldi et al. 1985; Flash 1987). These elastic properties of the motor system are essential for maintaining posture – the establishment of an appropriate mechanical impedance and equilibrium position for the limb is necessary to achieve stable limb postures and interactive behavior with the environment (Colgate 1988; Colgate and Hogan 1988). Our experiments have been directed toward understanding what factors affect the stiffness of the limb and what strategies are used by the central nervous system (CNS) to assure stability.

The specific function of multiarticular muscles in biological systems has not been established previously. Multijoint muscles are not necessary for the production of arbitrary force vectors by a two-joint arm; the necessary torque could be provided by the single-joint muscles alone. On the basis of theoretical work, Hogan argued that double-joint muscles could generate an endpoint stiffness of arbitrary shape and orientation (Hogan 1985), where the "shape" of the hand stiffness tensor is defined as the ratio of maximum to minimum stiffness and the "orientation" is given by the direction of maximum stiffness (Mussa-Ivaldi et al. 1985). However, experimental work shows that human motor system does not take advantage of this mechanical opportunity. Human subjects are not able to significantly alter either the shape or the orientation of the stiffness field at the hand (Flash and Mussa-Ivaldi 1990). Theoretical studies have shown that optimal trajectory execution with a fixed joint stiffness requires the presence of a significant level of double-joint stiffness (Flanagan et al. 1989).

The modeling and data described in this paper present a new view of the role of muscles which span two or

more joints. The presence of these muscles allows for the mechanical coupling of torque and stiffness across joints. Our findings indicate that, to achieve a passive stabilization of the limb through muscle mechanical properties, multijoint muscles must be present.

Stiffness and the control of posture

The static relationship between position and force defines the *elastic* behavior of a mechanism coupled with its environment. The stability of many mechanical systems can be assessed by examining this elastic behavior. The stiffness of a system can be described by the change in force exerted by the system on the environment in response to an externally imposed change in position at steady state. A system is *stable* if the induced force from the system has a component in the direction opposite to that of an imposed displacement. In contrast, a system is *unstable* if the induced force has a component in the same direction as the displacement.

For a nonlinear mechanical system, the overall elastic properties are not determined solely by spring-like elements of the system. Consider the example of a muscle spanning a single joint. As the joint is moved, the muscle is stretched or relaxed, changing the level of generated force. Thus, the muscle force is a function of the joint position. The torque produced by the muscle around the joint is a product of the force in the muscle times the moment arm of the muscle with respect to the joint. In general, the moment arm depends on the position of the joint. Thus, as the joint moves, the torque generated by the muscle will vary owing to the changing moment arm, as well as to force changes in the muscle itself.

To illustrate this mathematically, we can define the joint torque (τ) as a function of joint position (θ) and muscle force (f). We can then calculate what the stiffness (k_θ) of the system is with respect to joint rotations. In this expression, the moment arm [$j(\theta)$] varies according to the joint angle:

$$\tau(\theta) = j(\theta) f(\theta) \tag{1}$$

$$k_\theta = \frac{d\tau}{d\theta} \tag{2}$$

$$= \frac{dj(\theta)}{d\theta} f(\theta) + j(\theta) \frac{df(\theta)}{d\theta}. \tag{3}$$

Thus, the overall stiffness has two components, one reflecting the stiffness of the spring-like muscle and the other stemming from changes in moment arm depending on the joint position. This latter term depends on the actual force in the muscle at a given moment. The system is stable with respect to joint rotations if the total stiffness (i.e., the sum of the two components) is negative.

The concepts of stiffness and stability can be applied to a multidimensional mechanical system such as the human arm. Here we will focus on the stiffness and stability of a two-joint model of the arm. Displacements of the hand cause rotations at the joints, while torques at the joints produce linear forces at the hand. The mathematical description becomes a bit more complicated (force and displacements are represented by two-dimensional vectors and the stiffness becomes a two-by-two matrix), but the analysis is essentially the same as for the one-dimensional system described above – the overall stiffness of the system is determined by the nonlinear geometry of the mechanical linkage and the net force produced at the hand as well as the intrinsic elasticity of the muscles acting at the joints (see Appendix A).

The fact that hand stiffness depends on the net force produced by the arm is illustrated in Fig. 1. A posture is stable in multiple dimensions if a small displacement of the hand results in a change in force that acts to restore the original position. Figure 1A shows how the stiffness at the hand can be represented. Graphically, the stiffness is depicted as a local field of forces. The location of each arrow represents a displacement of the system from the center position, the same distance in each of the eight directions. The size and direction of each arrow corresponds to the size and direction of the change in force caused by that displacement. For a stable stiffness, all of the arrows must point inward. Mathematically, a necessary and sufficient condition for postural stability is that the stiffness matrix be negative definite. That is, all of the eigenvalues of the matrix must be less than zero (Ogata 1970). Thus, we can see whether a certain limb posture is stable by examining the characteristics of the measured stiffness field. We can quantify the stability by computing the eigenvalues of the estimated stiffness matrix.

Figure 1B shows the effect of a net force at the hand on the overall stiffness and stability of the system. We calculated what would be the stiffness at the hand for different net forces. (See the "constant joint stiffness" model in the Materials and methods section for details on this calculation.) The center field represents the stiffness of the endpoint for a particular value of joint stiffness operating against a zero force load. The surrounding fields illustrate what the measured endpoint stiffness would be for the arm in the same position with the same joint stiffness, but while producing a steady state force in the direction indicated by the large arrow. One can observe that (a) loads which cause the hand to *pull* (hand force directed toward either joint) tend to *stabilize* the limb, while (b) hand forces that *push* (away from the joints) tend to *destabilize* the limb. In fact, for this combination of force magnitude and joint stiffness, the hand stiffness is shown to be unstable for forces in certain directions (fields a and h).

An intuitive understanding of the source of the instability can be gained by comparing the two-joint arm system with a one-dimensional pendulum. Imagine a rigid link connecting the hand in a straight line to a pivot point at the shoulder (Fig. 1C). An external force acting inward along this line (i.e., the hand is pushing outward) would cause the system to behave like an inverted pendulum, generating an instability around the pivot point. Rotation around this pivot results in lateral motion of the

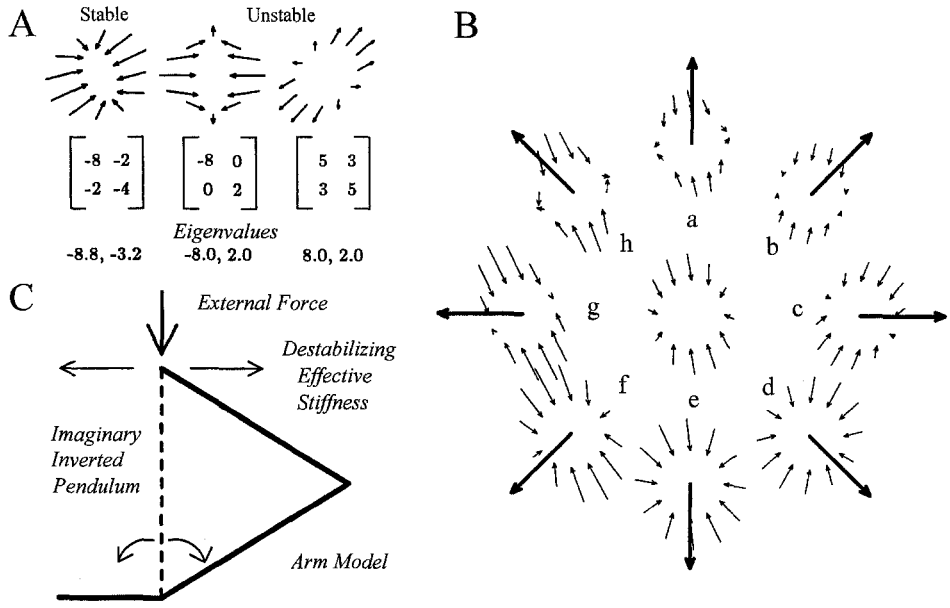

Fig. 1A–C Stiffness and stability of a two-joint arm. **A** Representations of two-dimensional stiffness. Stiffness can be represented mathematically by a matrix or graphically as a field of force vectors. Stability is determined by the eigenvalues of the stiffness matrix – for a stable system all eigenvalues must be negative. **B** Dependence of endpoint stiffness on output force direction. The center field represents the stiffness at the hand for a two-joint arm at a particular position and for a particular joint stiffness. Surrounding fields represent the hand stiffness for the arm in the same position, with the same joint stiffness, while producing a hand force in the direction of the *large arrow*. Note that the stiffness field can become unstable for forces in certain directions (*a*, *h*). **C** Source of endpoint instability. An intuitive understanding of the endpoint instability caused by an external force can be achieved by imagining an inverted pendulum between the hand and shoulder

endpoint. Thus, the effective stiffness generated by this geometrical effect produces instability at the hand perpendicular to the line of force. An applied force directed toward the pivot at the elbow would have a similar effect. In contrast, an applied force directed outward on the two-joint arm would make the system equivalent to a downward-oriented pendulum. Following the same arguments, such an applied force would tend to stabilize the system.

Control of stiffness and stability

A number of hypotheses can be formulated about how the CNS avoids instability while maintaining hand posture against force loads. Here we consider three possible control schemes:

Constant joint stiffness. One simple strategy, at least from a robotics point of view, is that of maintaining a constant joint stiffness independent of the output force. This strategy implies that the hand stiffness will change with the direction and magnitude of the external force. However, it is possible that the joint stiffness is high enough to maintain endpoint stability for loads of reasonable size. While we would not expect to see such a strategy in a biological system, where muscle and joint stiffness is known to vary with activation (Feldman 1966; Rack and Westbury 1969; Kearney and Hunter 1990), we tested this null hypothesis to see whether instability would be a problem in the absence of such stiffness variations. This analysis leads to insight as to why muscle stiffness may increase with muscle force.

Constant endpoint stiffness. A more complex strategy would be to control the joint stiffness so as to maintain a constant (and stable) endpoint stiffness. In this way the response of the system to force perturbations would be constant, independent of the level of force produced by the limb. At the task level, motor planning would be simplified. However, to maintain a constant endpoint stiffness, it is necessary to modify the joint stiffness as a function of the force load. As we will show, this strategy requires the coordination of stiffness level across multiple joints.

Passive stabilization. At each workspace location, a constant joint-stiffness strategy implies a predictable variation of the hand stiffness in relation to the applied load. In contrast, a constant endpoint-stiffness strategy implies a predictable variation of the joint stiffness. We simulated the two control strategies with a two-joint arm model. By comparing the results of the simulations to actual stiffnesses measures, we found that neither of these strategies captures the qualitative behavior of human subjects working against a static load. Therefore, we simulated a third control strategy, which we call *passive stabilization*, in which the hand stiffness is stabilized indirectly via the mechanical properties of the force-producing elements. This strategy is based on two assumptions arising from known experimental observations:

1. Muscle stiffness increases as the muscle force output increases (Feldman 1966; Rack and Westbury 1969; Hoffer and Andreassen 1981; Kearney and Hunter 1990).

2. Multiarticular muscles are active even when torque is produced only at a single joint (Buchanan et al. 1986; Jongen et al. 1989).

The motivation for this apparently ad hoc strategy came from the output of our earlier simulations and will be discussed in a later section.

The results of these simulation studies provided insight into issues concerning the stability of the human arm. These insights led us to develop hypotheses about how the CNS accomplishes this task. We tested these hypotheses experimentally by measuring the response of human subjects.

Materials and methods

We measured the stiffness of the human arm for subjects working against force loads, and we compared these measured responses with simulations of a two-joint arm. We measured the stiffness and stability for the arm in the horizontal plane and we limited our analysis to force loads acting in two directions along a single axis in the horizontal plane, as shown in Fig. 2. A positive force value corresponds to an outward push by the hand, while a negative force value signifies an inward pull. This position and force direction were chosen because they accentuate the problem of instability at the hand. In this position, no torque needs to be generated at the shoulder to achieve forces in the desired direction. Stability, however, will be strongly affected by positive force loads. Note that forces in nearby directions would have a similar effect on limb stability (see Fig. 1B). Thus, our results do not depend on the precise maintenance of this singular position.

Stiffness values were computed for force values of various magnitudes and in both directions (positive values correspond to the hand pushing, negative value correspond to pulling). The stiffness of the hand is displayed both graphically, as a set of force/displacement vectors, and in a plot of stiffness eigenvalues versus force load. For each condition, the joint stiffness is divided into three independent components, corresponding ideally to the contribution of each of the shoulder single-joint, elbow single-joint, and double-joint muscles to the overall joint stiffness (Fig. 2). These components are plotted separately against the applied force load (Figs. 4–10). This decomposition of joint stiffness was based on the simplifying assumption that the muscles act with constant moment arms at the joints. Furthermore, it was assumed that the moment arms of the double-joint muscles are equal for each joint (r_1/r_2=1). The dependence of the results upon these assumptions will be discussed in a subsequent section.

Simulation methods

Constant joint stiffness model. To simulate the response of a constant joint stiffness model, constant values were selected for each component of the stiffness matrix $\boldsymbol{K}_\Theta$. The equation

$$\mathbf{K}_X = \mathbf{J}^{-1^T}(\Theta)\left[\mathbf{K}_\Theta - \frac{\partial \mathbf{J}^T(\Theta)}{\partial \Theta}\mathbf{F}\right]\mathbf{J}^{-1}(\Theta) \tag{4}$$

was then used to compute the resulting hand stiffness $\mathbf{K}_x$ predicted for each applied force load, where $\mathbf{F}$ is the net force at the hand and $\mathbf{J}(\Theta)$ is the Jacobian of the coordinate transformation from joint angles to hand position. (See Appendix A for the derivation of Eq. 4 and a definition of all symbols.)

Constant hand stiffness model. In this case the values of the hand stiffness matrix were selected and assumed to be constant. Joint stiffness values were computed from the specified hand stiffnesses by inverting Eq. 4:

$$\mathbf{K}_\Theta = \mathbf{J}^T(\Theta)\mathbf{K}_X\mathbf{J}(\Theta) + \frac{\partial \mathbf{J}^T(\Theta)}{\partial \Theta}\mathbf{F} \tag{5}$$

Passive stabilization model. To simulate this strategy the muscle elastic response was modeled as an exponential relationship between muscle length and muscle force. This relationship satisfies the assumption that stiffness ($\partial f/\partial l$) increases with muscle force and is consistent with observed biological data (Feldman 1966; Rack and Westbury 1969; Kearney and Hunter 1990). While only an approximate representation of the force/length characteristics of muscle, the details of this relationship are not essential to the foregoing analysis. The important point is that muscle stiffness increases with muscle force. The torque required to produce a desired force output was distributed between the uniarticular and biarticular muscles based on the relative stiffness values of each. This is also in agreement with experimental observations (Buchanan et al. 1986; Jongen et al. 1989).

The imposed force load was used to compute the required muscle force under each simulated condition. The relationship between muscle force and stiffness was used to compute the resulting joint stiffness matrix, and Eq. 4 was once again used to compute the corresponding hand stiffness.

Experimental methods

Three normal, healthy volunteers, aged 25–35 years, participated in these experiments. The stiffness of the human arm was measured for each subject maintaining a specified posture against different force loads. Stiffness was measured statically using the methods of Mussa-Ivaldi et al. (1985). To summarize briefly, the subject was seated in a straight-back chair in front a planar, two-

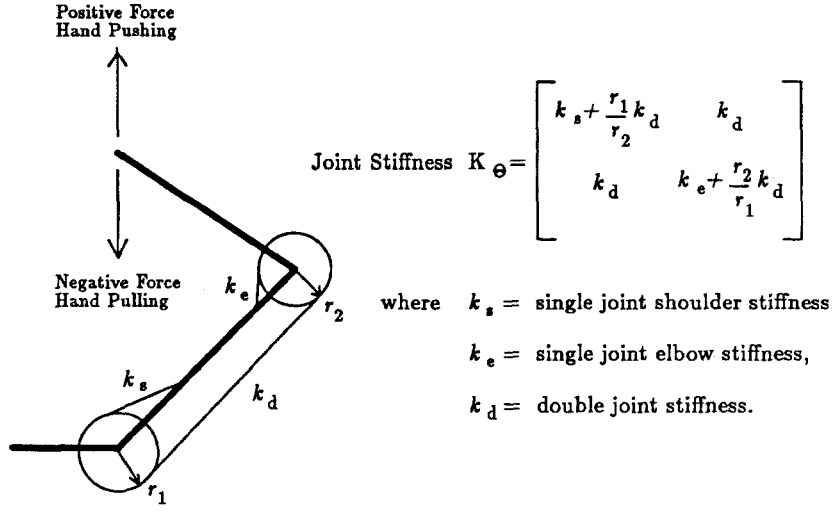

Fig. 2 Definition of joint stiffness components and force directions. The joint stiffness matrix $\mathbf{K}_\Theta$ is partitioned into three components: k_s, k_e, and k_d, corresponding to the combined stiffness (including both flexors and extensors) of the shoulder single-joint, elbow single-joint, and shoulder to elbow double-joint muscles, respectively

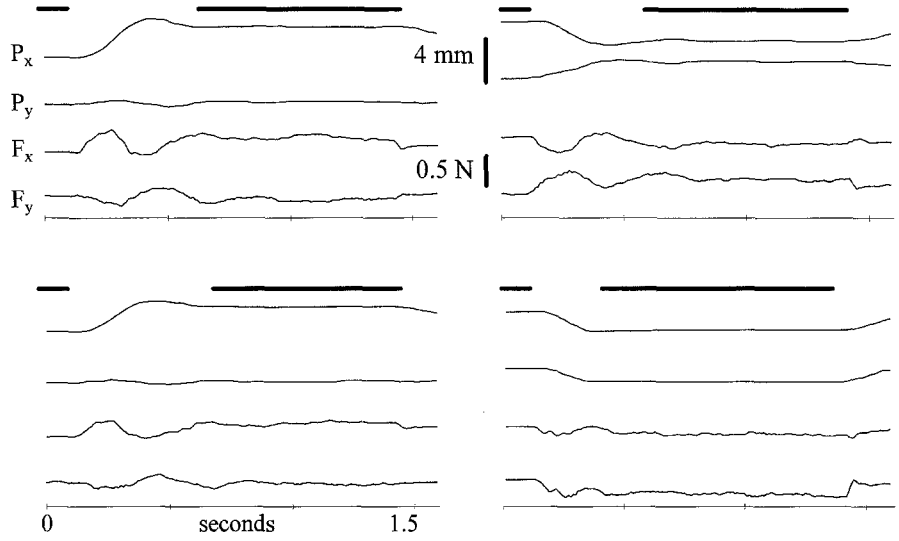

Fig. 3 Raw data records for four displacements from a single stiffness measurement. Two-dimensional hand position (P_x, P_y) and force (F_x, F_y) are plotted against time. The *bars* above each graph indicate the time periods over which the baseline and displaced data values were averaged. The net change in force and position was computed as the difference between two corresponding means. The net changes collected from 30 such displacements were used to estimate the two-dimensional joint stiffness at the hand

joint manipulandum. A strap around the torso of the subject and the chair prevented lateral movements of the shoulder with respect to the apparatus and the test position. Subjects grasped the handle of the manipulandum, the end of which was free to move in the horizontal plane. The subject's elbow was supported by a sling suspended from the ceiling, thus restricting the movement of the arm to the horizontal plane. A splint attached by Velcro straps to the hand and forearm prevented flexion at the wrist.

To initiate a trial, the subject was required to move the hand to the specified starting position 30 cm in front of and in line with the shoulder. This target location was indicated by a light-emitting diode (LED) suspended above the plane of the workspace. When the subject's hand was at rest within a small distance of the initial position, displacements were imposed on the hand through servo-control of torque motors acting at the two joints of the apparatus. Displacements of two different magnitudes and in eight directions were applied for each stiffness measurement. Actual displacements were measured by optical encoders at the joints of the apparatus and varied between 1 and 4 mm. The hand was gradually displaced over the course of 150 ms, held for 1.2 s, then released gradually over 150 ms. Subjects were instructed to not consciously intervene when the hand was displaced.

The forces required to move and hold the hand at the desired displaced position were measured by a six-axis force/torque transducer (Lord F/T series model 15/50; range ±66 N, resolution ±0.05 N) mounted on the handle of the manipulandum. (This is different from the original experiments by Mussa-Ivaldi et al. (1985), in which the forces were measured indirectly by the current in the servomotors). The force sensor was powered for at least 30 min prior to each experiment to avoid problems of thermal sensitivity. The subject was allowed to rest for several minutes between measurements at different loads and at any time he or she felt fatigued.

An off-line, automatic procedure was used to determine when the hand came to rest ($v<0.3$ cm/s) following the initiation of the servo displacement (typically after 600 ms). The X–Y forces and the actual achieved displacement from the the starting position were averaged over this period (300–800 ms). Linear regression of this data was used to compute a best fit, two-by-two matrix representing the stiffness field at the hand (Mussa-Ivaldi et al. 1985). Figure 3 shows raw data records for four different displacements from a single stiffness measurement.

The symmetric and antisymmetric components of the measured hand stiffnesses were compared for each subject, confirming that for the loads applied in this study the antisymmetric component contributes negligibly to the stiffness field (Mussa-Ivaldi et al. 1985). Only the symmetric component of this matrix was used in the subsequent analysis.

Force loads were generated by attaching various lead weights to the subject's hand via a cable and pulley arrangement, so as to produce a force along the line between the hand and the shoulder. The magnitude of the load was independently measured at the hand with a linear force transducer, to account for any friction in the pulley (which appeared to be negligible). While there was little or no intrinsic stiffness associated with the weight and cable, the geometry of the load apparatus generated a component of stiffness at the hand in the direction perpendicular to the direction of the cable (the cable/weight/pulley system is itself a nonlinear linkage). The stiffness of the load apparatus was computed for each force value and subtracted from the measured stiffness to get the intrinsic hand stiffness:

$$\mathbf{K}_{\text{load}} = -mg\begin{bmatrix}\left(\frac{1}{l}-\frac{x_p^2}{l^3}\right) & -\frac{x_p y_p}{l^3}\\ -\frac{x_p y_p}{l^3} & \left(\frac{1}{l}-\frac{y_p^2}{l^3}\right)\end{bmatrix} \tag{6}$$

$$\mathbf{K}_X = \mathbf{K}_{\text{measured}} - \mathbf{K}_{\text{load}} \tag{7}$$

where (x_p, y_p) is the location of the hand *with respect to the pulley*, $l=[x_p^2+y_p^2]^{-(1/2)}$ is the distance from the hand to the pulley, m is the mass of the weight, and g is the acceleration due to gravity. Seven to twelve different load values were applied, ranging from −60 to +60 N, following the convention of Fig. 2.

The actual joint stiffness matrix used by the subject was computed from each measured hand stiffness and force load by Eq. 5. Limb dimensions (interjoint distances) were measured simply with a ruler. Measured hand stiffnesses were plotted as vector fields, along with the stiffness eigenvalues and computed joint stiffness components for each measurement. (Not all of the measured stiffness values are plotted as vector fields.)

The experimentally measured stiffness properties were compared with four different models of stiffness control. For each model and each subject we fit the free parameters of the model to the measured data and then used the model to predict the system behavior for various force loads.

First, a constant joint stiffness model was computed, based on the joint stiffness computed from the measured hand stiffness for the subject at rest (zero force load):

$$\hat{\mathbf{K}}_\Theta(\mathbf{F}) = \mathbf{K}_\Theta(0) \tag{8}$$

where $\hat{\mathbf{K}}$ represents the values produced by the model. Equation 4 was used to compute the model hand stiffness $\hat{\mathbf{K}}_X(\mathbf{F})$.

A second constant joint stiffness model was also fit to each set of data, this time using the mean joint stiffness computed from measurements for all force loads. This produces the "best fit" constant joint stiffness model:

$$\hat{\mathbf{K}}_\Theta(\mathbf{F}) = \frac{1}{n}\sum_{i=1}^{n}\mathbf{K}_\Theta(\mathbf{F}_i) \tag{9}$$

where $F_1 \ldots F_n$ represent each of the tested force load values.

A model of constant hand stiffness was fit to each set of data:

$$\hat{\mathbf{K}}_X(\mathbf{F}) = \frac{1}{n}\sum_{i=1}^{n}\mathbf{K}_X(\mathbf{F}_i) \tag{10}$$

Equation 5 was used to compute the required model joint stiffnesses $\hat{\mathbf{K}}_\Theta(\mathbf{F})$ for each applied force.

Finally, a model of increasing joint stiffness versus force load was tested. Linear regression was used to produce functions relating the joint stiffness values to the magnitude of the applied load. Separate linear functions were fit for each of the joint stiffness components $\hat{k}_s$, $\hat{k}_e$, and $\hat{k}_d$. The regression parameters for each subject are presented in Appendix B. These components were then combined to produce the model joint stiffness matrix $\hat{\mathbf{K}}_\Theta$ as in Fig. 2.

The predicted output of the models was compared with the measured and computed data. The error between the predictions and the data is defined as:

$$\varepsilon = \mathbf{K}_X - \hat{\mathbf{K}}_X \tag{11}$$

Defining the norm of a matrix to be equal to its largest eigenvalue (Strang 1989), the mean magnitude of the error matrices ε_i for a given model was used as a measure of its fit to the data.

Simulations and analyses were performed on a Symbolics 3600 Lisp Machine using the algorithms described in previous publications (McIntyre 1990; McIntyre et al. 1989).

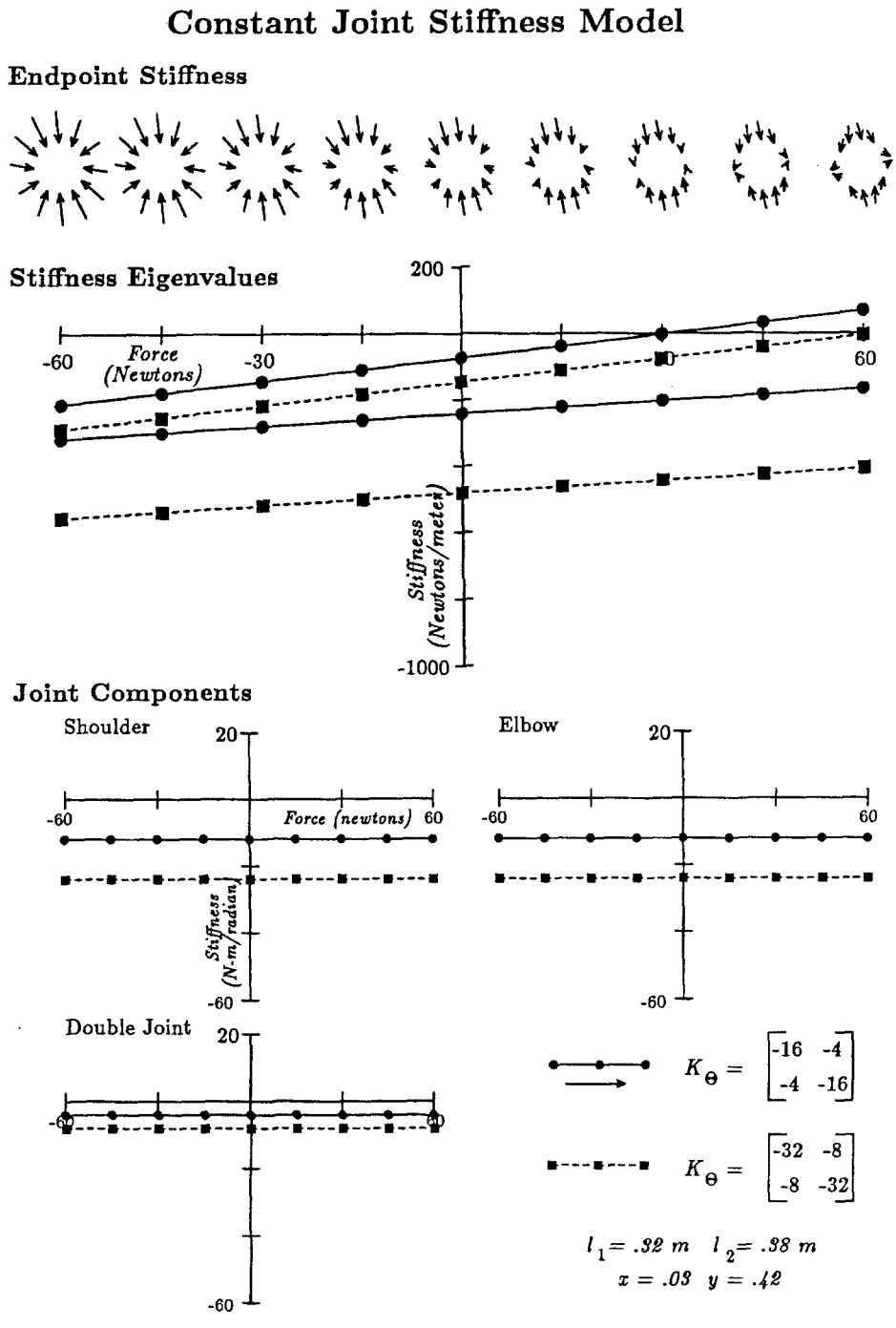

Fig. 4 Simulation of constant joint stiffness control for low (*solid*) and high (*dashed*) levels of joint stiffness. The *top line* shows the effective hand stiffness as a function of force load, in a vector field representation. The *middle graph* shows the variation of the two hand stiffness eigenvalues as a function of force load (one line per eigenvalue for each level of joint stiffness). The *lower graphs* show the values of each joint stiffness component. The eigenvalues of the hand stiffness matrix can become positive, demonstrating that if the joint stiffness is held constant the hand stiffness can become unstable at sufficiently high loads

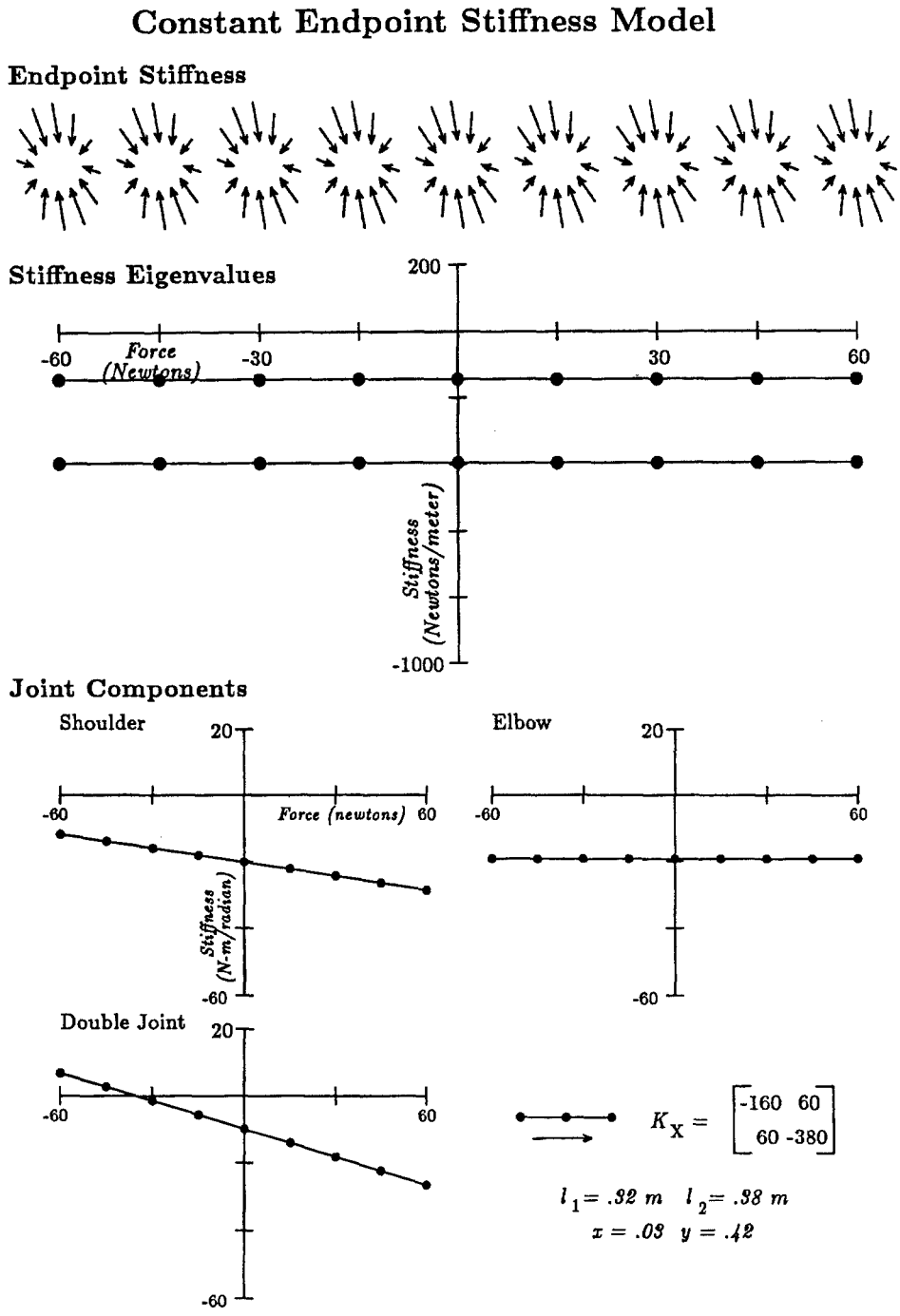

Fig. 5 Simulation of constant endpoint stiffness control. Shoulder and double-joint muscles must stiffen in order to maintain a constant stiffness at the hand

Results

To gain insight into the control problem, we first considered the simulations of the proposed control strategies. We then compared these models with the measured data from human subjects.

Simulation results

Constant joint stiffness. Figure 4 shows the hand stiffnesses resulting from a constant joint stiffness control strategy for two different values of joint stiffness. The lower-magnitude joint stiffness is typical of a human subject acting against a zero force load. The endpoint stiffness was computed for conditions in which the limb maintains the same posture and joint stiffness while producing a desired output force. The fields along the top of the figure represent the predicted stiffnesses for nine different specified force loads using the lower magnitude of joint stiffness. Below these figures is plotted a graph of the eigenvalues of the computed stiffness matrices. This plot shows that if the arm were to maintain a low constant joint stiffness (solid lines) the endpoint stiffness would become unstable at approximately 30 N force. The system can be stabilized to a greater magnitude of

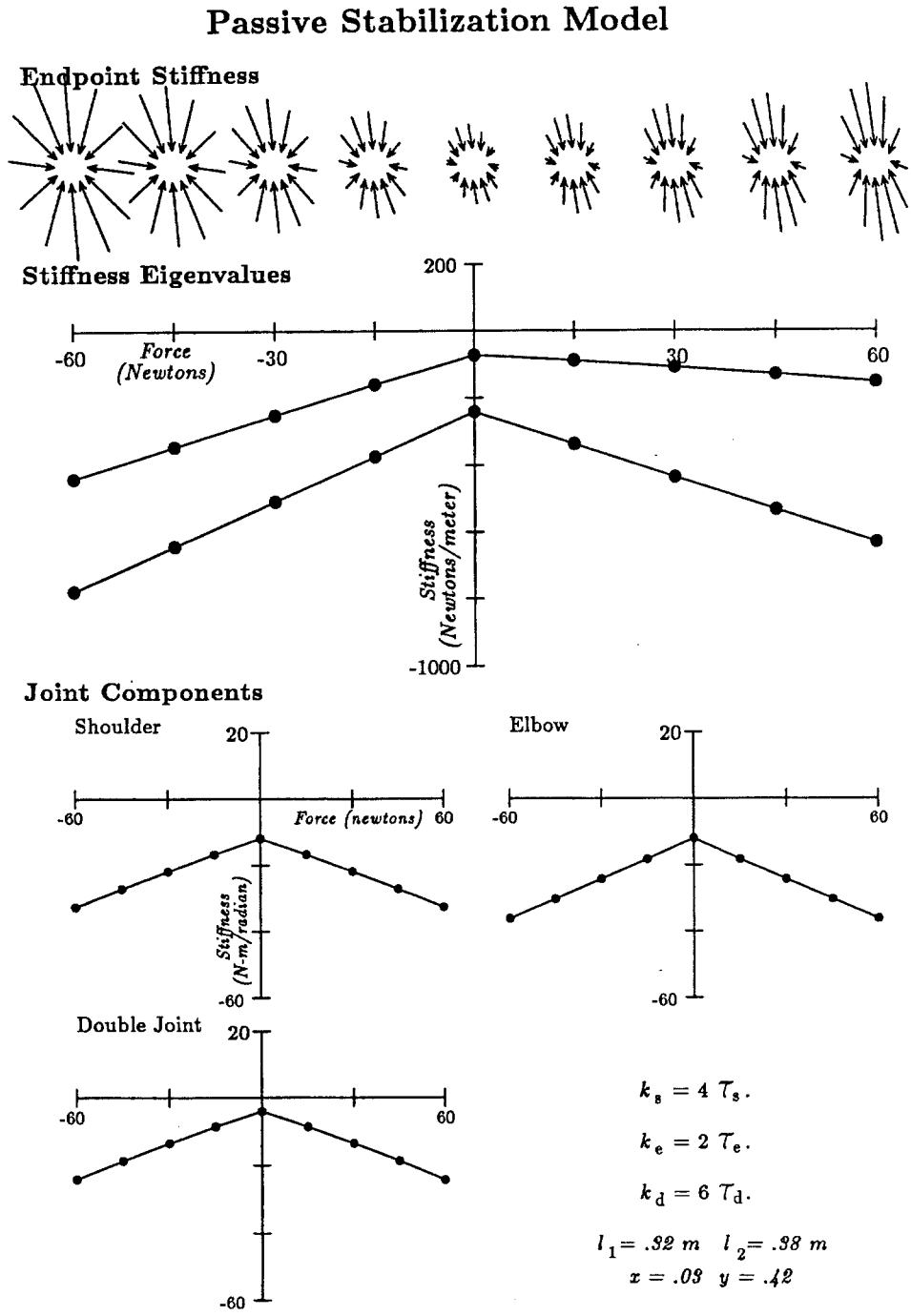

Fig. 6 Arm stiffness for the passive stabilization strategy using an exponential model of muscle. Hand stiffness is not constant, but stability is maintained

applied force if a higher constant joint stiffness is used (dashed lines).

Constant endpoint stiffness. Figure 5 shows the joint stiffness values required to produce a constant endpoint stiffness. Looking at the plots of joint components versus force, this figure shows that the shoulder and double-joint stiffness components must vary with the hand force in order to maintain a constant hand stiffness. This is interesting, because, for force loads in these two directions, there is no torque being produced at the shoulder (the line of force passes through the shoulder; see Fig. 2). In order to maintain a constant endpoint stiffness, *shoulder* stiffness must increase in response to an increase in torque at the *elbow*. Equally significant is the fact that elbow stiffness need not increase in this case in order to maintain stability.

Passive stabilization. The proposed passive stabilization strategy was based on the assumption of increasing muscle stiffness with muscle force, and the contribution of double-joint muscles to the production of torque at the elbow. The importance of these two conditions is apparent from the previous examples. Joint stiffness must increase (become more negative) with the force load in certain directions in order to maintain hand stability. Fur-

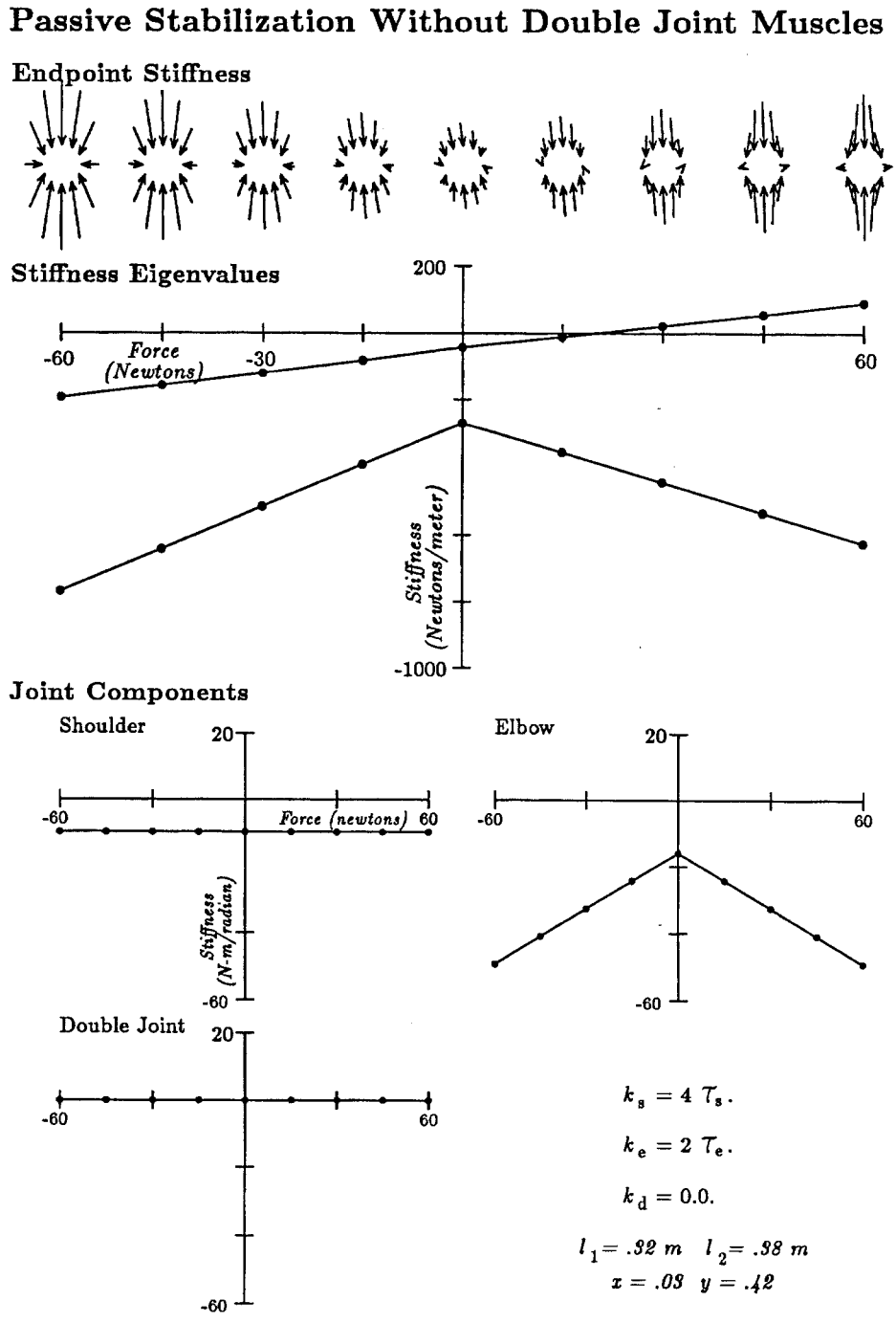

Fig. 7 Exponential muscle model without double-joint muscles. Without the stiffening action of the double-joint muscles, stability is not maintained

thermore, torque production at one joint must be coupled with stiffness changes at another. As torque is produced to generate the desired force, increases in muscle stiffness would produce the necessary change in joint stiffness, while multijoint muscles would provide the required interjoint coupling.

Figure 6 shows the hand stiffness obtained from a system having muscles that stiffen proportionally with output force. Unlike the constant joint stiffness model, stability is maintained despite increases in force load. The mechanics by which the hand stiffness is stabilized are apparent in the plot of the joint stiffness components. As the force load increases, the torque at the elbow must increase. According to our assumptions (see Materials and methods, and Discussion), this torque load is shared by the single-joint elbow and double-joint muscles. The increase in double-joint muscle force generates an increase in stiffness at both joints. In addition, because the double-joint muscle produces torque at both the shoulder and the elbow, the single-joint shoulder flexors must become active in order to counteract the shoulder torque. The resulting increase in stiffness of the single-joint shoulder muscles further stabilizes the limb.

In contrast to the constant endpoint stiffness model, the stiffness at the elbow also increases owing to the increase in elbow single-joint muscle activity. Further-

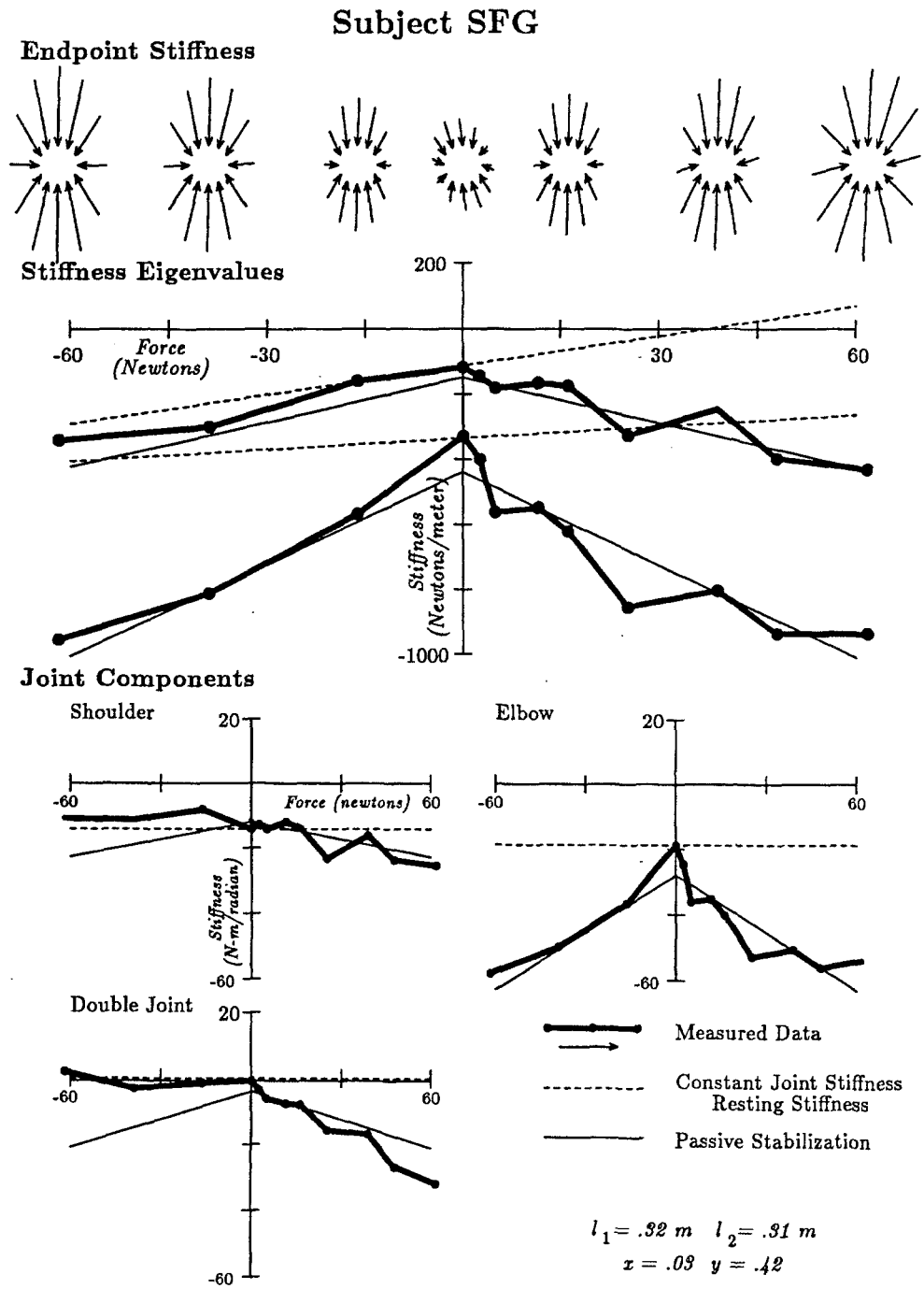

Fig. 8 Stiffness data for subject S.F.G. The *dashed lines* indicate the predicted response for the constant joint stiffness model. The *solid lines* show the response of the best-fit passive stabilization model

more, the double-joint stiffness increases for hand forces in the negative direction as well. Each of these effects tends to increase the overall stiffness of the hand. The endpoint stiffness will indeed change for different force loads, but the fundamental condition of stability will be satisfied.

The double-joint muscles play a key role in stabilizing the limb under this strategy. To emphasize this point, Fig. 7 shows the hand stiffnesses generated by a simulated two-joint arm having only single-joint muscles. The stiffness at the elbow increases with the level of force output, but since the shoulder muscle generates no torque, there is no change in shoulder stiffness. The pattern of endpoint stiffness is different from the constant joint stiffness model, however the stiffness can still become unstable as the force level increases.

Model predictions. The predictions that can be made from these control models are summarized as follows:

1. Maintaining a constant joint stiffness will yield a destabilization of the hand stiffness when operating against certain force loads, possibly to the point of instability.
2. Stabilizing the hand stiffness requires the coupling of torque changes at one joint with stiffness changes at another.

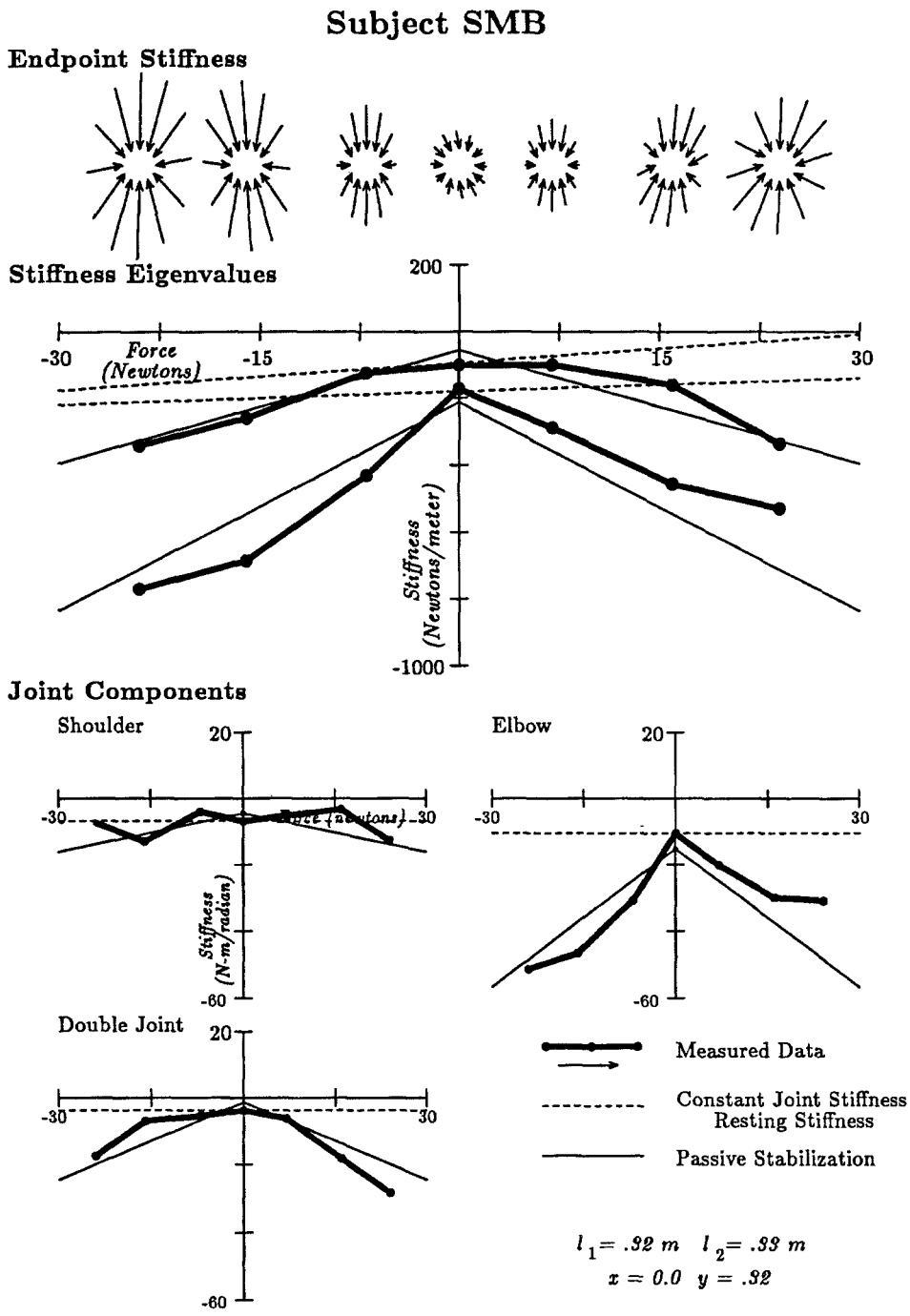

Fig. 9 Stiffness data for subject S.M.B

3. A local strategy in which muscle stiffness increases with output force can effectively stabilize the limb.
4. Multiarticular muscles provide the interjoint coupling necessary to stabilize the limb.

For nonlinear linkages, such as a two-joint arm, stability depends on the force output. A system which controls such a linkage must take into account this dependence. We have examined how the human motor system controls limb stiffness under varying load conditions, and compared the response of the subjects with that of the proposed control models described above.

Experimental results

The stiffness parameters for each of the three subjects are plotted in Figs. 8–10. The measured hand stiffness did not become unstable for any subject under any of the force loads tested, as evidenced by the negative eigenvalues for each of the measured stiffness matrices. In fact, each subject showed a trend toward increasing stability (more negative eigenvalues) as the magnitude of the force load increased. In all cases the magnitude of the double-joint stiffness component increased as a function of force load.

Lines representing the simulated results for the constant joint stiffness control model are superimposed on

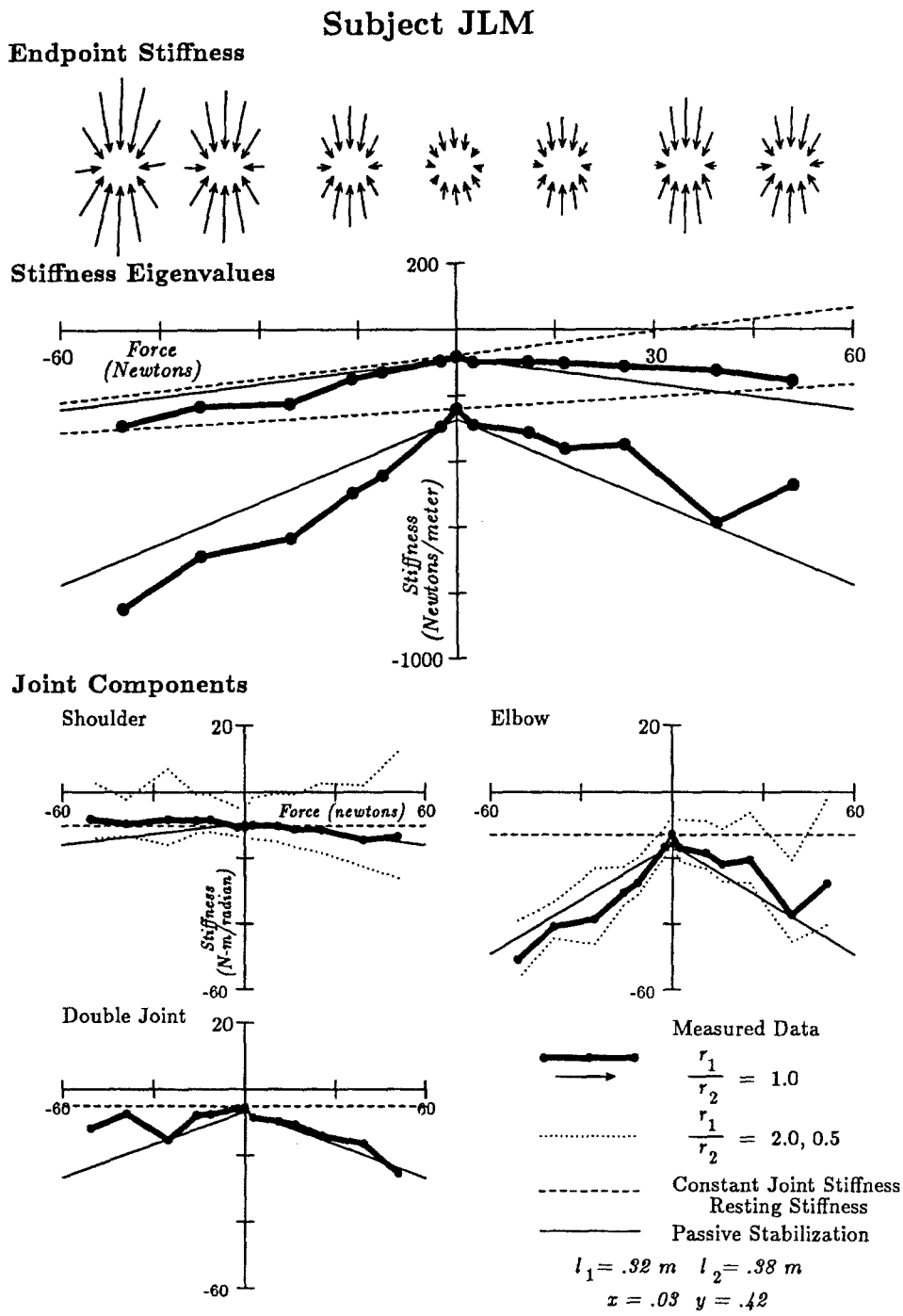

Fig. 10 Stiffness data for subject J.L.M. The sensitivity of the joint stiffness calculation to changes of the assumed double-joint muscle moment arm ratios is also shown

the plots of the measured stiffness values. The simulation of a constant joint stiffness predicts a positive (unstable) hand stiffness eigenvalue for loads above approximately 30 N. From these simulations one can see that a constant joint stiffness strategy would produce an unstable hand stiffness at force loads within the range achieved by subjects S.F.G. and J.L.M. Subject S.M.B. was not tested above the potentially unstable level of force, but showed no trend toward becoming unstable within the tested range.

We wished to test the statistical validity of this result. For a single measured parameter, we would normally compute an ideal value at which the system would become unstable, then perform an appropriate statistical test to show that the measured values are significantly different from this threshold. We cannot, however, compute threshold values for each joint stiffness component, because the stability of the system depends on the particular combination of all three. Instead, we tested the variability of the joint stiffness values computed from measured data, defined confidence limits for the true mean of these values, and then showed that, for joint stiffness components within these ranges, the system would become unstable.

The hand stiffness was sampled on subject S.F.G. five times each at a load of 0 N and 2.5 N, and the mean of

Table 1 Comparison of control models

	Mean error for different control models			
	Constant joint stiffness		Constant endpoint stiffness	Exponential muscle model
	Rest stiffness	Best fit		
S.F.G.	409	210	197	84
J.L.M.	233	144	149	88
S.M.B.	319	195	193	107

each component of the hand stiffness was computed. Assuming a *t*-distribution of each joint stiffness component around the true mean, the 99% confidence interval for the true joint stiffness values can be computed:

$$\hat{\mathbf{K}}_{\Theta}|_{F=0}\begin{bmatrix} -178 < \mathbf{K}_{xx} < -85 & 5 < \mathbf{K}_{xy} < 81 \\ 42 < \mathbf{K}_{yx} < 94 & -474 < \mathbf{K}_{yy} < -154 \end{bmatrix}$$

$$\hat{\mathbf{K}}_{\Theta}|_{F=2,5}\begin{bmatrix} -169 < \mathbf{K}_{xx} < -120 & -17 < \mathbf{K}_{xy} < 45 \\ -3 < \mathbf{K}_{yx} < 83 & -515 < \mathbf{K}_{yy} < -154 \end{bmatrix}$$

We then allow each independent joint stiffness value (maintaining a symmetric matrix, as in our previous computations) to assume the most stable (most negative) value within its respective range, i.e.,

$$\hat{\mathbf{K}}_{\Theta} = \begin{bmatrix} -178 & -17 \\ -17 & -515 \end{bmatrix}$$

Computation of the hand stiffness using this joint stiffness levels shows that if the arm were to maintain a constant joint stiffness at this level, the hand stiffness would become unstable at one or more of the test force loads.

The likelihood that the true mean for a given value would be more negative than its respective limit is less than 0.005 (one-tailed test). If measurement error in all four components varied independently, the likelihood that all four would reach this limit is very small (0.005^4); however, we expect error in these values to covary, since we are computing four values from raw data having only two degrees of freedom (F_x and F_y). On the other hand, even if errors in all four components covaried exactly, the odds that the true joint stiffness is this negative are still only 0.005. By this overly conservative estimate, we can be sure of the reliability of these results.

The four control models produce different predictions for the hand and joint stiffnesses measured for different force loads. Table 1 presents the quantitative comparison of each of the simulated models with the measured data. For all three subjects the best model was that of increasing muscle stiffness with output force.

Discussion

It is immediately clear from the Cartesian representation of the measured stiffness that subjects did not become unstable under any of the force loads tested. This is demonstrated by the fact the the subjects were able to maintain the required posture during measurement of the hand stiffness. Had they become unstable, it would have been impossible for the subject to perform even this simple task. The question is not *whether* but *how* the arm remains stable in the presence of a load.

Our experimental results rule out the hypothesis that the CNS controls the limb so as to maintain either a constant joint stiffness or a constant endpoint stiffness. The constant joint stiffness model would predict a monotonic change in the effective hand stiffness with respect to the applied force, which would become unstable at sufficiently high loads. A model in which the endpoint stiffness is held constant would require a monotonic increase in shoulder and double-joint stiffnesses, and no change in elbow stiffness. None of these predictions are in agreement with the qualitative features of the observed data.

The data are in better agreement with the passive stabilization model for the control of stability. Subjects maintain stability, demonstrating that coupling is occurring between the shoulder and elbow, since no shoulder torque is required. The fact that the elbow stiffness goes up dramatically with elbow torque, *even though this is not required to maintain stability*, is consistent with this model for the control of stiffness. Furthermore, the double-joint stiffness is seen to increase with hand force, in particular for forces in the positive (destabilizing) direction. This supports the notion that the double-joint muscles are involved in the cross-joint coupling required for overall limb stability.

The predictions of the passive stabilization model do not exactly match all the qualitative features of the measured data. In the measured data the increase in stiffness seen for each of the joint components is asymmetric with respect to the direction of force. In fact, in some cases the shoulder and double-joint stiffness components appear to be relatively constant for negative (stabilizing) forces. This is in contrast to the symmetric patterns of stiffness change predicted by the passive stabilization model (Fig. 6). In this model, however, torques and stiffnesses were produced by ideal spring-like actuators acting at the joints, one for each of the joint components. In reality, the joint torques are produced by agonist/antagonist groups of muscles. The torque produced in one particular direction is generated by a different set of muscles than for torque in the opposite direction, e.g., triceps is activated to generate a pushing force, while the biceps is used for pulling. Thus, it is reasonable to expect a different stiffness versus torque relationship for forces in different directions. On the other hand, this may be evidence for stiffness adaptation according to the nature of the load. Shoulder and double-joint stiffness may be increased only for destabilizing loads.

Flash, Mussa-Ivaldi and colleagues (Flash and Mussa-Ivaldi 1990) have previously investigated the hand stiffness and the joint stiffness of the multijoint arm in subjects who maintained the hand at a number of locations in the horizontal plane. In this study it was found that subjects have a limited ability to modulate either the shape or the orientation of the hand stiffness field. Only

the size varied in response to various force perturbations. The current results do not contradict these observations, even in the presence of high force loads. Neither the measured hand stiffnesses nor the passive stabilization model show a significant change in the shape or the orientation of the hand stiffness as the force increases, because the eigenvalues of the stiffness matrix tend to covary. In contrast, however, passive stabilization without double-joint muscles would show a substantial change in the shape of the stiffness field. Thus, while subjects may not be able to exploit fully the two-joint muscles to produce arbitrary stiffness field shapes and orientations, the presence of double-joint muscles helps to provide more uniform hand stiffness properties.

Role of double-joint muscles

The current study presents a new view of the role of multijoint muscles. In terms of joint torques, the destabilizing effect of the endpoint force is a global property of the system resulting from the nonlinear nature of the linkage. The level of torque being produced at one joint can affect the stiffness required at the other. If either joint were studied in isolation, or if pure torque loads were used, the effects on stabiliy could not be observed. Yet the human motor system can adopt a local strategy for controlling stability. With multijoint muscles present, each muscle stiffness need be a function only of its own force output in order to maintain overall limb stability. The multiarticular muscles provide the necessary coupling between joints. This is an example of a mechanical design simplifying the control problem.

Mechanical properties, reflexes and voluntary responses

Our experiments have not addressed the question of how the changes in joint stiffness are achieved. A particularly elegant solution arises from the fact that muscles stiffen as the force increases (Hoffer and Andreassen 1981). In this way, stiffness control would be achieved with no additional intervention from the nervous system. This is the essence of the "passive stabilization" model that we have presented.

One should note, however, that the intrinsic stability arising from a fixed relationship between stiffness and output force is not adequate to solve all postural control problems. For example, Hogan (1984) found an experiental condition under which load stabilization was achieved through cocontraction at the elbow. In his single-joint task, no net change in torque was required to support the change in load, so passive stabilization via increased force output would not have been adequate to maintain stability. A similar strategy might be employed under the force conditions of the current study. External force loads might induce the subject to cocontract muscles at the shoulder to increase the joint stiffness without a net generation of torque.

A third possibility exists: joint stiffness could increase through changes in the reflex feedback gains which contribute to the stiffness around the joint (Nichols and Houk 1976). In this case it would be the reflex gains of the shoulder single-joint muscles along with, perhaps, the double-joint muscles that would be expected to increase.

Finally, we cannot rule out a voluntary response on the part of the subject, despite instructions to avoid them. Previous experiments in which electromyographic (EMG) signals were measured indicate that subjects indeed do not respond "voluntarily" (Mussa-Ivaldi et al. 1985). Furthermore, the hand did come to rest at some distance from the target position when the displacement was applied to the hand. The subject could presumably cancel the imposed perturbation by a voluntary action, as the forces produced by the motors were not excessive. In any case, even if a voluntary response is involved, the control of the hand position still exhibits spring-like properties. A more fundamental issue is that of mechanical versus neuronal effects.

Unfortunately, we are unable to distinguish between these possibilities, based on our experimental results. We can see from the fits of the passive stabilization model that shoulder stiffness increases for destabilizing loads in all subjects (shoulder stiffness vs force slopes are nonzero). This is consistent with all three hypothetical models presented above. The measurement of force changes after the limb has come to rest prevents us from distinguishing between muscle mechanical properties and reflex effects. In the case of the passive stabilization model, this increase in shoulder single-joint stiffness comes from the need to activate single-joint shoulder flexors to counteract the shoulder torque generated by the double-joint extensors. While not conclusive, the fact that double-joint stiffness increases more than shoulder stiffness favors the passive stabilization model.

Muscle length-tension properties

In the simulations of the increasing muscle stiffness model, a linear force-stiffness relationship was used to model the muscle response. Other nonlinear relationships between stiffness and force would also be sufficient to guarantee stability, the key assumption is only that stiffness must increase with muscle force. From Eq. 4 we can see that the overall stability of the limb is determined by the sum of two factors, the stabilizing effect of the joint stiffness plus the potentially destabilizing effect of the load coupled with the nonlinear geometry of the mechanical system. The destablilizing effect of the applied load increases linearly with the force magnitude, as does the joint torque required to counteract the load. If at any given force level the increase in stability provided by changes in joint stiffness is greater than the instability due to the nonlinear geometry and load, the system will remain stable.

Data from Hoffer and Andreassen suggest that a linear increase in stiffness versus force is characteristic of

areflexive muscle (Hoffer and Andreassen 1981). In the presence of reflexes, the increase in muscle stiffness is steeper for low levels of force and flattens out at high levels. This relationship between force and stiffness can still provide for stabilization of the limb, provided that the average rate of stiffness increase is sufficiently high for the entire useful range of muscle forces.

Distribution of muscle activity

For a given force at the hand, there is no uniquely defined set of muscle activations. In the simulations we assumed that the double-joint muscles contributed to the hand forces that were produced. Specifically, we distributed the load proportionally according to the relative stiffness of each muscle. Passive stabilization of the limb through muscle mechanical properties does not imply necessarily this specific rule for the distribution of muscle activity, but it does require that the double-joint muscles participate in torques produced at either joint. Measurements of EMG signals during production of torques in the human arm support this assumption (Gielen and van Zuylen 1986; Jongen et al. 1989).

The values estimated from measured data suggest that perhaps the rule we used in the simulations for distributing muscle forces does not reflect what is done by the CNS. For stabilizing loads, the shoulder and double-joint stiffness components do not increase, in contrast to the model predictions. This may simply be due to different elastic properties for the flexor and extensor double-joint muscle groups, as noted above. On the other hand, it may reflect a difference in the relative activation of two-joint muscles depending on the destabilizing effect of the load. A refinement of the passive stabilization model might include a consideration of force direction in the distribution of muscle forces, predicting a higher participation by multijoint muscles for destabilizing loads.

Model parameters

We now consider how these results are affected by the specific choice of mechanical parameters in our simulations and experiments.

Equal moment arms. The computation of joint stiffness components was based on the assumption that the double-joint muscles act at each joint with equal moment arms (r_1/r_2=1). This assumption can be relaxed without altering the conclusions, since neither the observed hand stiffness values nor the overall joint stiffness matrix is affected by this assumption. The conclusion that the subject maintains neither a constant hand stiffness nor a constant joint stiffness are valid regardless of the value of r_1/r_2.

Variations in the value of r_1/r_2 affect only the relative contribution of each type of muscle to the overall joint stiffness. Figure 10 shows the joint stiffness components computed for subject J.L.M. using three different values for the moment arm ratio. These values span the range of reasonable real values for the moment arm ratio. The change in ratio quantitatively affects the shoulder and elbow components, but qualitatively the results are the same. The elbow stiffness continues to increase for forces in either direction. The values for the double-joint stiffness components are unaffected by the choice of the moment arm ratio.

Constant moment arms. For the analysis of the measured data, we assumed that the muscles acted at the joints with constant moment arms and attributed observed changes in joint stiffness to changes in muscle stiffness. A muscle acting with a nonconstant moment arm around a joint would produce an effective joint stiffness component dependent on both the intrinsic muscle stiffness and the muscle force. Such an effective joint stiffness would depend very much on the position of the limb at the time. It is conceivable that the observed changes in joint stiffness can be attributed solely to this mechanical effect, but it is unlikely that it would be sufficient to stabilize the limb in all areas of the workspace.

Nominal hand position and force direction. In these experiments we chose to study the effect of force loads that were directed between the hand and the shoulder. This singular configuration was chosen because it most strongly demonstrates the need for coupling between the two joints. This alignment of forces through the shoulder is not essential, however, as shown by Fig. 1. Loads over a wide range of directions have a destabilizing effect on the hand stiffness. Torques at the shoulder would increase only slightly for small deviations from this alignment. For a 1-cm lateral deviation from this line, a 1-N load at the hand would require a 1-Ncm torque at the shoulder, and approximately a 22-Ncm torque at the elbow. Thus, the shoulder torque will still be relatively small, while significant shoulder stiffening will still be required. Thus, our results are insensitive to small errors in the initial positioning of the hand and to the displacements imposed by the stiffness measuring procedure.

Conclusions

To adequately control the stability of a multijoint limb, the force being produced by the limb must be considered. These experiments have shown that for human subjects joint stiffness must increase with force output in order to maintain stability at the hand.

A model of stiffness control has been proposed in which limb stability is maintained through the intrinsic mechanical properties of the system. This strategy is biologically plausible and the competence of the model has been demonstrated by computer simulations. The stability of the limb is a global property of the motor system, depending on limb configuration and net output force. The proposed model, on the other hand, is entirely based

on local processing of information, in which a muscle's stiffness depends only on that muscle's force output. The ability of this local strategy to stabilize the hand results from the mechanical coupling provided by the two-joint muscles of the arm, suggesting a precise role for multiarticular muscles in the control of limb posture.

In human subjects, the CNS maintains neither a constant joint stiffness nor a constant endpoint stiffness when faced with different forces. Of the control models tested, stiffness control in human subjects is best described by the passive stabilization of the endpoint through increasing muscle stiffness and the action of multijoint muscles.

Acknowledgements This work was supported by a Whitaker Health Science Fund predoctoral fellowship to J. McIntyre, and by NIH grants NS09343 and AR26710 and ONR grant N00014/88/K/0372 to F.A. Mussa-Ivaldi and E. Bizzi.

Appendix A: derivation of stiffness and stability

Stiffness and stability can be defined as follows: for a one-dimensional system, if the force output of the device is described at steady state by the function

$$f=g(x) \tag{A1}$$

the *stiffness* as a function of position is given by

$$k(x)=\frac{dg}{dx} \tag{A2}$$

A system can be considered stable around a position x_1 if the value of the stiffness at that point is negative [$k(x_1)<0$]; a positive stiffness means the system is unstable. Note that the stability of a nonlinear system having zero stiffness at a given point cannot be determined by looking at the stiffness value alone (Ogata 1970).

For multidimensional systems, the position of the system and the force acting on the system are described by n-dimensional vectors **X** and **F**. If the force acting on the system is described by a vector function **G**,

$$\mathbf{F}=\mathbf{G}(\mathbf{X}) \tag{A3}$$

the stiffness of the system is an elastic tensor represented by the n by n matrix

$$\mathbf{K}=\begin{bmatrix} \frac{\partial F_1}{\partial X_1} & \cdots & \frac{\partial F_1}{\partial X_n} \\ \vdots & \ddots & \vdots \\ \frac{\partial F_n}{\partial X_1} & \cdots & \frac{\partial F_n}{\partial X_n} \end{bmatrix} \tag{A4}$$

A necessary and sufficient condition for postural stability is that **K** be negative definite. That is, all the eigenvalues of **K** must be less than zero (Ogata 1970).

For a two-joint arm we define the following symbols: Θ, vector of joint angles; $\mathbf{K}_\Theta$, 2×2 joint stiffness matrix; τ, vector of joint torques; $\mathbf{K}_x$, 2×2 hand stiffness matrix; **X** Cartesian position of hand; **J** 2×2 Jacobian matrix; **F** Force output at hand.

The relationship between hand and joint stiffness is derived as follows:

$$\mathbf{K}_\Theta=\frac{\partial \tau}{\partial \Theta} \tag{A5}$$
$$\tag{A6}$$

Similarly, the *hand stiffness* relates the force to displacement vectors as measured at the hand:

$$\mathbf{K}_X=\frac{\partial \mathbf{F}}{\partial \mathbf{X}} \tag{A7}$$
$$\tag{A8}$$

To show this dependence, we can mathematically derive the hand stiffness equation as follows. The position of the hand (**X**) is a function of the joint angle vector (Θ):

$$\mathbf{X}=f(\Theta) \tag{A9}$$

The Jacobian matrix $\mathbf{J}(\Theta)$ relates small changes in tip position to changes in joint angles:

$$J(\Theta)=\frac{\partial f}{\partial \Theta} \tag{A10}$$

$$d\mathbf{X}=\mathbf{J}(\Theta)d\Theta \tag{A11}$$

The torque required to produce a given tip force is (Brady et al. 1983):

$$\tau=\mathbf{J}^T(\Theta)\mathbf{F} \tag{A12}$$

The relationship between joint and hand stiffness can then be derived by differentiating Eq. A12 (see Mussa-Ivaldi et al. 1989):

$$\mathbf{K}_\Theta=\frac{\partial \tau}{\partial \Theta} \tag{A13}$$

$$=\mathbf{J}^T(\Theta)\frac{\partial \mathbf{F}}{\partial \Theta}+\frac{\partial \mathbf{J}^T(\Theta)}{\partial \Theta}\mathbf{F} \tag{A14}$$

$$=\mathbf{J}^T(\Theta)\mathbf{K}_X\mathbf{J}(\Theta)+\frac{\partial \mathbf{J}^T(\Theta)}{\partial \Theta}\mathbf{F} \tag{A15}$$

$$\mathbf{K}_X=\mathbf{J}^{-1^T}(\Theta)\left[\mathbf{K}_{(\Theta)}-\frac{\partial \mathbf{J}^T(\Theta)}{\partial \Theta}\mathbf{F}\right]\mathbf{J}^{-1}(\Theta) \tag{A16}$$

The term

$$\frac{\partial \mathbf{J}^T(\Theta)}{\partial \Theta}\mathbf{F}$$

reflects the effective stiffness resulting from the position dependence of the Jacobian. It is computed as follows:

$$\gamma_{ij}\hat{=}\left[\frac{\partial \mathbf{J}^T(\Theta)}{\partial \Theta}\mathbf{F}\right]_{ij}=\sum_k \frac{\partial [\mathbf{J}^T(\Theta)]_{jk}}{\partial \Theta_i}\mathbf{F}_k=\sum_k \frac{\partial^2 \mathbf{X}}{\partial \Theta_i \partial \Theta_j}\mathbf{F}_k \tag{A17}$$

From Eq. A16 it can be seen that the stiffness at the hand depends not only on the value of the joint stiffness $\mathbf{K}_\Theta$ but also on the position Θ and *tip force* **F**.

Under the conditions of zero force load (**F**=0), Eq. A16 reduces to

$$\mathbf{K}_X=\mathbf{J}^{-1^T}(\Theta)\mathbf{K}_\Theta\mathbf{J}^{-1}(\Theta) \tag{A18}$$

If $\mathbf{K}_\Theta$ is negative definite (has all negative eigenvalues and is therefore stable), then $\mathbf{K}_X$ is also negative definite (stable) regardless of the value of $\mathbf{J}(\Theta)^{-1}$ (Strang 1980).

In the presence of a force load, a stable joint stiffness is no longer sufficient to guarantee limb stability. At high enough loads, the stiffness term

$$\frac{\partial \mathbf{J}^T(\Theta)}{\partial \Theta}\mathbf{F}$$

of Eq. A16 can significantly affect the hand stiffness tensor. For a two-joint limb, loads directed away from a joint center tend to stabilize the limb, while loads directed toward a joint have a destabilizing effect.

Appendix B: Best-fit model parameters

Subject	Constant joint rest stiffness $\hat{\mathbf{K}}_\Theta$	Constant joint best fit $\hat{\mathbf{K}}_\Theta$	Constant endpoint stiffness $\hat{\mathbf{K}}_X$	Exponential muscle model
S.E.G.	$\begin{bmatrix} -14.9 & -0.7 \\ -0.7 & -19.5 \end{bmatrix}$	$\begin{bmatrix} -25.4 & -9.9 \\ -9.9 & -52.7 \end{bmatrix}$	$\begin{bmatrix} -251.5 & -16.0 \\ -16.0 & -690.3 \end{bmatrix}$	$\hat{k}_s = -0.183F - 11.8$ $\hat{k}_e = -0.583F - 28.1$ $\hat{k}_d = -0.284F - 3.9$
J.L.M	$\begin{bmatrix} -15.4 & -5.11 \\ -5.11 & -18.0 \end{bmatrix}$	$\begin{bmatrix} -21.6 & -11.2 \\ -11.2 & -38.9 \end{bmatrix}$	$\begin{bmatrix} -145.7 & -5.9 \\ -5.9 & -461.0 \end{bmatrix}$	$\hat{k}_s = -0.111F - 9.4$ $\hat{k}_e = -0.555F - 16.0$ $\hat{k}_d = -0.334F - 6.70$
S.M.B.	$\begin{bmatrix} -10.9 & -3.9 \\ -3.9 & -14.5 \end{bmatrix}$	$\begin{bmatrix} -20.0 & -12.4 \\ -12.4 & -43.9 \end{bmatrix}$	$\begin{bmatrix} -210.3 & -3.8 \\ -3.8 & -469.3 \end{bmatrix}$	$\hat{k}_s = -0.385F - 4.6$ $\hat{k}_e = -1.38F - 15.1$ $\hat{k}_d = -0.774F - 1.40$

References

Brady M, Hollerbach JM, Johnson TL, Lozano-Perez T, Mason MT (eds) (1983) Robot motion: planning and control. MIT Press, Cambrige, Mass

Buchanan TS, Almdale DPJ, Lewis JL, Rymer WZ (1986) Characteristics of synergic relations during isometric contractions of human elbow muscles. J Neurophysiol 56:1225–1241

Colgate JE (1988) The control of dynamically interacting systems. PhD thesis, MIT, Cambridge, Mass

Colgate JE, Hogan N (1988) Robust control of dynamically interacting systems. Int J Control 48:65–88

Feldman AG (1966) Functional tuning of nervous system with control of movement or maintenance of a steady posture. III. Mechanographic analysis of the execution by man of the simplest motor task. Biophysics 11:766–775

Flanagan JR, Feldman AG, Ostry DJ (1989) The equilibrium point model for two-joint arm movement control. Soc Neurosci Abstr 15:173

Flash T (1987) The control of hand equilibrium trajectories in multi-joint arm movements. Biol Cybern 57:257–274

Flash T, Mussa-Ivaldi FA (1990) Human arm stiffness characteristics during the maintenance of posture. Exp Brain Res 82:315–326

Gielen CCAM, Zuylen EJ van (1986) Coordination of arm muscles during flexion and supination: application of the tensor analysis approach. Neuroscience 17:527–539

Hoffer JA, Andreassen S (1981) Regulation of soleus muscle stiffness in premammillary cats: intrinsic and reflex components. J Neurophysiol 45:267–285

Hogan N (1984) Adaptive control of mechanical impedance by coactivation of antagonist muscles. IEEE Trans Autom Control 29:681–690

Hogan N (1985) The mechanics of multi-joint posture and movement control. Biol Cybern 52:315–351

Jongen HAH, Denier van der Gon JJ, Gielen CCAM (1989) Activation of human arm muscles during flexion/extension and supination/pronation tasks. Biol Cybern 61:1–9

Kearney RE, Hunter IW (1990) System identification of human joint dynamics. CRC Crit Rev Biomed Eng 18:55–87

McIntyre J (1990) Utilizing system elastic properties for the control of posture and movement. PhD thesis, MIT, Cambridge, Mass

McIntyre J, Mussa-Ivaldi FA, Bizzi B (1989) Modelling of multijoint motor systems. Proc Annu Int Conf IEEE Eng Med Biol Soc 11:242–243

Mussa-Ivaldi FA, Hogan N, Bizzi E (1985) Neural, mechanical and geometric factors subserving arm posture in humans. Neuroscience 5:2732–2743

Mussa-Ivaldi FA, Morasso P, Hogan N, Bizzi E (1989) Network models of motor systems with many degrees of freedom. In: Fraser MD (ed) Advances in control networks and large scale parallel distributed processing models. Ablex, Norwood

Nichols TR, Houk JC (1976) Improvement in linearity and regulation of stiffness that results from actions of the stretch reflex. J Neurophysiol 39:119–142

Ogata K (1970) Modern control engineering (Electrical engineering series) Prentice-Hall, Englewood Cliffs, NJ

Rack PMH, Westbury DR (1969) The effects of length and stimulus rate on the tension in the isolated cat soleus muscle. J Physiol (Lond) 204:443–460

Strang G (1980) Linear algebra and its applications. Academic, New York